Structure factor determination of amorphous materials by neutron diffraction

2008 J. Phys.: Condens. Matter 20 244109

(http://iopscience.iop.org/0953-8984/20/24/244109)

IOP PUBLISHING JOURNAL OF PHYSICS: CONDENSED MATTER

J. Phys.: Condens. Matter **20** (2008) 244109 (9pp) doi:10.1088/0953-8984/20/24/244109

Structure factor determination of amorphous materials by neutron diffraction

Gabriel J Cuello

Institut Laue Langevin, 6 rue Jules Horowitz, BP 156, F-38042 Grenoble Cedex 9, France

E-mail: cuello@ill.eu

Received 27 February 2008
Published 29 May 2008
Online at stacks.iop.org/JPhysCM/20/244109

Abstract

An introduction is given to structure factor determination by means of neutron diffraction. The method of isotopic substitution, which allows us to separate the partial correlation functions, is also presented. Suitable instruments, the experimental procedures, and corrections are described. Other less-conventional techniques such as isomorphic substitution and anomalous dispersion are also discussed. Finally, examples of the structure factor determination in chalcogenide, molecular, telluride and phosphate glasses are discussed in order to illustrate the usefulness of the neutron diffraction technique.

(Some figures in this article are in colour only in the electronic version)

1. Introduction

In this paper an elementary introduction to the method of structure factor determination by neutron diffraction will be given. In particular, it will focus on the structural characterization of amorphous materials. In an ideal case, the structure of a given system is completely determined when one is able to know the equilibrium position of all atoms. This is quite straightforward in the case of crystalline solids, for which these equilibrium positions are not only well defined but also periodically repeated. For these systems the diffraction experiments produce diffractograms with the characteristic Bragg reflexions evidenced by well defined thin peaks at given angular positions, corresponding to the scattering vector matching a vector in the reciprocal lattice.

In the case of an amorphous material, there are no longer clearly defined equilibrium positions. Instead of having well defined atomic positions, one must refer to a distribution of atoms as a function of distance, i.e. to the probability of finding an atom at a distance r provided there is another atom at the origin. The so-called pair distribution function $g(r)$ is proportional to this probability and it is the function that one usually intends to obtain from the experiment. A schematic example of this function is shown in figure 1, where the main characteristics of a general pair distribution function are evident. Firstly, this function must be strictly zero below a given distance, because of the atomic repulsion between atoms.

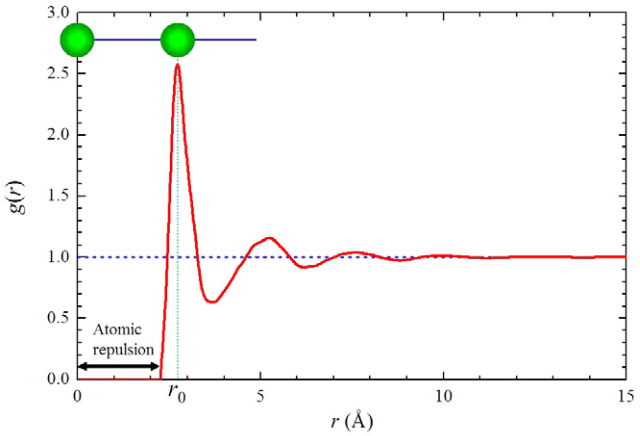

Figure 1. Schematic pair distribution function. This function must be null below a given distance related to the atomic repulsion, and the position of the first maximum (r_0) corresponds to the minimum in the pair potential.

Secondly, the function should exhibit alternating maxima and minima following the so-called coordination shells. Finally, the oscillations should be more or less damped (for a less or more ordered system, respectively) and should tend to unity for long distances, where the correlation with the atom at the origin is completely lost.

The objective of this article is to show how to obtain this function from the experimentally determined intensity as a function of the scattering vector. Section 2 will be devoted to the fundamentals of neutron diffraction. In section 3 we shall discuss some of the experimental issues that we usually face to extract the correlation functions, and we shall present the available instruments suited for structural studies on amorphous materials. Finally, in section 4 we shall discuss examples where these methods have been successfully applied to give an insight into the structure of glassy systems.

2. Fundamentals

In a standard scattering experiment, we measure the intensity as a function of the scattering angle 2θ (or time of flight in the case of pulsed sources) and energy exchange $\hbar\omega$, related to the double differential cross section as follows:

$$I(2\theta,\omega) = C\Phi_0\epsilon(k')\frac{\mathrm{d}^2\sigma}{\mathrm{d}\Omega \mathrm{d}\omega}(2\theta,\omega), \tag{1}$$

where $C\Phi_0$ represents the flux of incident particles (neutrons) and C is a normalization constant; $\epsilon(k')$ represents the efficiency of the detection device. This cross section is itself related to the microscopic properties of the system,

$$\frac{\mathrm{d}^2\sigma}{\mathrm{d}\Omega\,\mathrm{d}\omega}(2\theta,\omega) = N\frac{k'}{k}\frac{\sigma}{4\pi}S(\vec{Q},\omega), \tag{2}$$

where N is the number of scatterer particles; $\vec{k}$ and $\vec{k}'$ are the initial and final wavevectors of the probing particles ($\vec{Q} = \vec{k} - \vec{k}'$ is the scattering vector); σ is the scattering cross section; and finally, $S(\vec{Q},\omega)$ is the dynamical structure factor, the magnitude which contains all the information about the structure and dynamics of the system.

2.1. Monatomic systems

For a set of N identical atoms of a general system, we are able to obtain the dynamical structure factor if we know the position of all atoms, $\vec{r}_i(t)$ with $i = 1,\ldots,N$, for all times.

$$S(\vec{Q},\omega) = \frac{1}{2\pi}\int_{-\infty}^{+\infty}\mathrm{d}t\,\mathrm{e}^{-\mathrm{i}\omega t}\frac{1}{N}\sum_{i,j}^{N}\left\langle \mathrm{e}^{-\mathrm{i}\vec{Q}\cdot\vec{r}_i(0)}\mathrm{e}^{-\mathrm{i}\vec{Q}\cdot\vec{r}_j(t)}\right\rangle, \tag{3}$$

where the brackets represent the thermal average over the scatterer centers. The microscopic density of the system can be expressed as the sum of Dirac's deltas centered on each scatterer,

$$\rho(\vec{r},t) = \sum_{i=1}^{N}\delta\left(\vec{r} - \vec{r}_i(t)\right). \tag{4}$$

Then, the dynamic structure factor is

$$S(\vec{Q},\omega) = \frac{1}{2\pi}\int\int \mathrm{d}\vec{r}\,\mathrm{d}t\,\mathrm{e}^{\mathrm{i}(\vec{Q}\cdot\vec{r}-\omega t)}G(\vec{r},t), \tag{5}$$

where the function $G(\vec{r},t)$ is a time-dependent correlation function (the Van Hove correlation function) [1], which is related to the probability of finding a particle at position $\vec{r}$ and time t, provided that another particle was at the origin at $t = 0$. This correlation function can be written as a function of the microscopic density

$$G(\vec{r},t) = \frac{1}{N}\int \mathrm{d}\vec{r}'\left\langle \rho(\vec{r}',0)\rho(\vec{r}+\vec{r}',t)\right\rangle. \tag{6}$$

The double differential cross section can be separated into two terms

$$\frac{\mathrm{d}^2\sigma}{\mathrm{d}\Omega\,\mathrm{d}\omega}(2\theta,\omega) = N\frac{k'}{k}\left(\frac{\sigma_{\mathrm{coh}}}{4\pi}S(\vec{Q},\omega) + \frac{\sigma_{\mathrm{incoh}}}{4\pi}S(\vec{Q},\omega)\right), \tag{7}$$

the coherent part containing all the correlations, and the incoherent one just containing the auto-correlations (an atom with itself). The latter gives information on diffusive motions and internal dynamics (molecular vibrations). The inelastic part of the coherent term gives information about collective dynamics, and the elastic part contains the structural information. These cross sections, $\sigma_{\mathrm{coh}} = 4\pi b_{\mathrm{coh}}^2$ and $\sigma_{\mathrm{incoh}} = 4\pi b_{\mathrm{incoh}}^2$, can be calculated from the tabulated values for the scattering lengths [2]. In this work we are focused in the structure of the system and the only important term is the coherent one.

In diffraction experiments the detectors integrate all the neutrons regardless of their energy exchanges with the sample, i.e. there is no discrimination in the final energy. In mathematical language, this is equivalent to integrating the dynamical structure factor over all energies, so

$$S(\vec{Q}) = \int_{-\infty}^{+\infty}\mathrm{d}\omega\,S(\vec{Q},\omega) = \int \mathrm{d}\vec{r}\,\mathrm{e}^{\mathrm{i}\vec{Q}\cdot\vec{r}}G(\vec{r},0). \tag{8}$$

In fact, from the experimental point of view, this is an approximation (the so-called static approximation) because of the reduced energy exchange in a real experiment. Under this approximation, the correlation function is evaluated at $t = 0$, which is equivalent to a snapshot of the system. In this case, the correlation function has a very simple expression; it is just $G(\vec{r},0) = \delta(\vec{r}) + \rho g(\vec{r})$, i.e. a delta function at the origin representing the autocorrelation plus the space-dependent density variations.

Then the static structure factor can be easily calculated,

$$S(\vec{Q}) = 1 + \rho\int \mathrm{d}\vec{r}\,\mathrm{e}^{\mathrm{i}\vec{Q}\cdot\vec{r}}g(\vec{r}) \tag{9}$$

or written in a slightly different way,

$$S(\vec{Q}) - 1 = \rho\int_V \mathrm{d}\vec{r}\left[g(\vec{r}) - 1\right]\mathrm{e}^{\mathrm{i}\vec{Q}\cdot\vec{r}}, \tag{10}$$

where we have subtracted a null term representing no scattered neutrons. These neutrons just pass through the sample without any interaction and they are not registered by the detector.

It is useful to define the structure factor as $F(\vec{Q}) = S(\vec{Q}) - 1$ and the pair correlation function as $G(\vec{r}) = 4\pi\rho r[g(\vec{r}) - 1]$; the function $F(\vec{Q})$ is the Fourier transformation of $G(\vec{r})/4\pi r$,

$$F(\vec{Q}) = \int_V \mathrm{d}\vec{r}\,\frac{G(\vec{r})}{4\pi r}\mathrm{e}^{\mathrm{i}\vec{Q}\cdot\vec{r}}, \tag{11}$$

and vice versa,

$$\frac{G(\vec{r})}{4\pi r} = \frac{1}{(2\pi)^3}\int \mathrm{d}\vec{Q}\, F(\vec{Q})\mathrm{e}^{-\mathrm{i}\vec{Q}\cdot\vec{r}}. \tag{12}$$

Here it is worth noticing that the pair correlation function $G(\vec{r})$ is not exactly the Van Hove's correlation function $G(\vec{r}, 0)$ and they should not be confused with each other. The relationship between these two functions is $G(\vec{r}, 0) = \delta(\vec{r}) + \rho + G(\vec{r})/4\pi r$.

In terms of the static structure factor and the pair distribution function, this can be written as

$$\rho\left[g(\vec{r}) - 1\right] = \frac{1}{(2\pi)^3}\int \mathrm{d}\vec{Q}\left[S(\vec{Q}) - 1\right]\mathrm{e}^{-\mathrm{i}\vec{Q}\cdot\vec{r}}. \tag{13}$$

As usual in disordered systems, it can be assumed that the scattering is isotropic and the three-dimensional Fourier transformations can be reduced to one-dimensional sine transformations as follows:

$$QF(Q) = \int_0^\infty G(r)\sin(Qr)\,\mathrm{d}r \tag{14}$$

and

$$G(r) = \frac{2}{\pi}\int_0^\infty QF(Q)\sin(Qr)\,\mathrm{d}Q. \tag{15}$$

In terms of the isotropic versions of the static structure factor and the pair distribution function, these integrals can be written as

$$S(Q) - 1 = \frac{4\pi\rho}{Q}\int_0^\infty r\,\left[g(r) - 1\right]\sin(Qr)\,\mathrm{d}r \tag{16}$$

and

$$g(r) - 1 = \frac{1}{2\pi^2\rho r}\int_0^\infty Q\,[S(Q) - 1]\sin(Qr)\,\mathrm{d}Q. \tag{17}$$

Figure 2 shows a real example of the structure factor and its corresponding pair distribution function for a binary alloy ($Al_{0.878}Si_{0.122}$) at 1373 K (i.e. in the liquid state). At a first glance, one can see that the structure factor goes to unity for high Q values, as predicted by equation (16). Using mechanical statistics arguments, it can be shown that $\rho k_B T \chi_T$ is the low-Q limit for the structure factor [4], where χ_T is the isothermal compressibility. These two limiting values are very useful for normalization purposes to obtain correct values for coordination numbers. There are some key features in the structure factor which can be translated easily to the pair distribution function. The position of the first intense diffraction peak Q_p in $S(Q)$ is related to the period $(2\pi/Q_p)$ of oscillations in the real space, i.e. with the spacing of the coordination shells. For this example, the position of the first diffraction peak is (2.67 ± 0.03) Å^{-1}, corresponding to a period in the real space of 2.35 Å, which must be compared with the experimental value of ≈2.4 Å. The width of this peak, ΔQ_p, gives information on the coordination length $(2\pi/\Delta Q_p)$, i.e. to what extent the system is ordered. In this case the width of the first peak is 0.75 Å^{-1}, giving a coordination length of ≈8.5 Å^{-1}, which matches very well with the damping of the oscillations in the pair distribution function (see figure 2(b)). This $g(r)$ function has been obtained by Fourier transformation of the structure factor following equation (17). As expected, it tends to unity for long distances, where the density fluctuations have lost all correlation with the reference atom at the origin. For very short distances, where a null function is expected, some small oscillations appear; they are not related to real correlations, but are produced because of the finite Q-range of any real experiment. These oscillations can be reduced using window functions as will be discussed later, but small oscillations in this region give an assessment of the goodness of the experimental data.

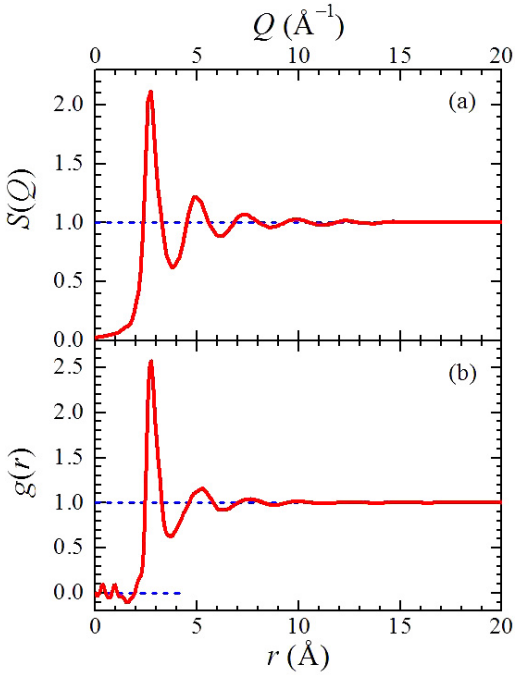

Figure 2. (a) The static structure factor of an AlSi liquid alloy as obtained from neutron diffraction experiments [3]. (b) The corresponding pair distribution function as obtained by Fourier transformation of the structure factor.

When working with correlation functions in real space, there are other related functions that are very useful. One of them is the pair correlation function $G(r) = 4\pi\rho r[g(r) - 1]$, the one-dimensional version of that defined by equation (11). Figure 3(b) plots the pair correlation function corresponding to the $g(r)$ plotted in part (a) of the same figure. It is worth noticing that $G(r)$ is a density-independent function (i.e. the knowledge of the density is not necessary to derive this function from experimental data), but provides an easy way to measure the density of the system (this function is also known as the density function). Due to the fact that $g(r)$ must be null in the repulsion region, $G(r)$ must have a linear dependence on r and the slope must be proportional to the density; in the case of the example shown in figure 3(b) the slope corresponds to an atomic density of 0.050 54 atoms Å^{-3}. This property is very useful when the sample is maintained under extreme conditions (e.g. high pressure or high temperature [5, 6]) and the conventional methods for density determination cannot be applied.

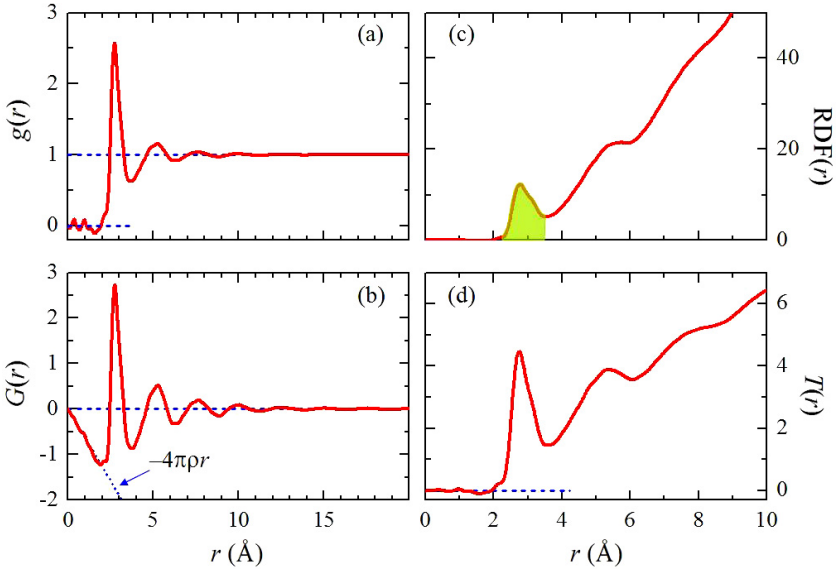

Figure 3. Correlation functions in real space. (a) Pair distribution function $g(r)$; (b) pair correlation function $G(r)$; (c) radial distribution function RDF(r); (d) $T(r) = 4\pi\rho r g(r)$.

The radial distribution function $\mathrm{RDF}(r) = 4\pi\rho r^2 g(r)$ is the number of atoms per unit length on the surface of a sphere of radius r. With such a definition, the integral of this function directly gives the number of atoms in a given coordination shell (the coordination number), as shown in figure 3(c). Occasionally it is better to use the function $T(r) = \mathrm{RDF}(r)/r$, which produces more symmetrical peaks, allowing the use of Gaussians as the functional shape for fitting the coordination shells (figure 3(d)).

2.2. Multiatomic systems

In the case of a system constituted of n different atomic species, the structure factor can be generalized as follows:

$$\bar{b}^2 F(Q) = \sum_{\alpha=1}^{n}\sum_{\beta=1}^{n} c_\alpha c_\beta b_\alpha b_\beta F_{\alpha\beta}(Q), \tag{18}$$

where $F_{\alpha\beta}(Q)$ are the partial static structure factors ($n_\mathrm{e} = n(n+1)/2$ independent functions in total) and $\bar{b}$ is the mean value of the coherent scattering length

$$\bar{b}^2 = \sum_{\alpha=1}^{n}\sum_{\beta=1}^{n} c_\alpha c_\beta b_\alpha b_\beta. \tag{19}$$

The main problem that an experimentalist should face is the fact that all the partial structure factors are added up in the same expression, i.e. a single diffractogram is measured containing all the partials that one would like to extract individually. To solve the problem, a set of n_e independent linear equations is needed. From a mathematical point of view, the problem can be solved just by changing the coefficients in equation (18), but in fact this must done carefully. If the compositions, c_α, change, the sample is changing, and this is unacceptable. The only possibility is changing the scattering length included in the weighting factors. This can be done using the technique of isotopic substitution under the assumption that the structural properties of the system are not changed by changing isotopes. There is also the possibility of using the technique of anomalous dispersion when one of the elements in the system has a resonance in the appropriate energy range, as has been recently shown [7, 8].

The linear system (18) can always be expressed as a matricial equation, $\vec{F}_\mathrm{S}(Q) = \mathbb{A}\vec{F}_\mathrm{P}(Q)$, where $\mathbb{A}$ is a $n_\mathrm{e} \times n_\mathrm{e}$ matrix and $\vec{F}_\mathrm{S}(Q)$ and $\vec{F}_\mathrm{P}(Q)$ are two vectors of n_e components, containing the independent measured structure factors and the partial correlations, respectively. As an example, for a binary system $n_\mathrm{e} = 3$ and equation (18) has the form

$$\bar{b}^2\begin{pmatrix} F_{\mathrm{S}1}(Q) \\ F_{\mathrm{S}2}(Q) \\ F_{\mathrm{S}3}(Q) \end{pmatrix} = \begin{pmatrix} c_\alpha^2 b_{\alpha1}^2 & c_\beta^2 b_{\beta1}^2 & 2c_\alpha c_\beta b_{\alpha1} b_{\beta1} \\ c_\alpha^2 b_{\alpha2}^2 & c_\beta^2 b_{\beta2}^2 & 2c_\alpha c_\beta b_{\alpha2} b_{\beta2} \\ c_\alpha^2 b_{\alpha3}^2 & c_\beta^2 b_{\beta3}^2 & 2c_\alpha c_\beta b_{\alpha3} b_{\beta3} \end{pmatrix} \times \begin{pmatrix} F_{\alpha\alpha}(Q) \\ F_{\beta\beta}(Q) \\ F_{\alpha\beta}(Q) \end{pmatrix}, \tag{20}$$

where $F_{\mathrm{S}1}(Q)$, $F_{\mathrm{S}2}(Q)$, $F_{\mathrm{S}3}(Q)$ are the measured structure factors for three different isotopic compositions of the same system, and $F_{\alpha\alpha}(Q)$, $F_{\beta\beta}(Q)$, $F_{\alpha\beta}(Q)$ are the sought partial structure factors.

Because the matrix $\mathbb{A}$ must be inverted, its determinant $\mathbb{A}$ is an important parameter which should be considered when the experiment is designed: the bigger the determinant, the smaller the uncertainties in the final results. Bigger values of this determinant are obtained by choosing isotopes with good contrast, i.e. with appreciably different scattering lengths (see [2]), or combining neutron and x-ray diffraction data [9].

Using equation (18) and the Fourier transformation (15), it is possible to generalize the expressions for the correlation functions in real space. In particular, the total correlation function $G(r)$ can be written in terms of the partials $G_{\alpha\beta}$, and

the expression is equivalent to equation (18) where F functions are replaced by G functions.

Even when isotopes are available, it is not always possible to prepare all the samples required to obtain the complete set of correlation functions. This is particularly true for systems with more than two atomic species. In this case we can apply the first difference method with isotopic substitution. If only one element can be substituted (γ), we can write equation (18) for each of the two samples: one with the $\gamma 1$ isotope and the other with the $\gamma 2$ isotope. Taking the difference between these two equations, all the correlations where the substituted atom is not included are canceled. In this way, we can write the following expression for the first difference spectrum:

$$\frac{\bar{b}^2 \Delta F_\gamma(Q)}{c_\gamma^2 (b_{\gamma 1}^2 - b_{\gamma 2}^2)} = F_{\gamma\gamma}(Q) + \frac{\sum_{\alpha \neq \gamma}^{n} c_\alpha b_\alpha F_{\alpha\gamma}(Q)}{c_\gamma (b_{\gamma 1} + b_{\gamma 2})}, \qquad (21)$$

where it has been possible to separate the γ–γ correlation and the second term is usually small.

Under given circumstances it is possible to perform a second substitution, the atomic species δ, for example. Then equation (21) can be re-written isolating the γ- and δ-correlations, for the two isotopes $\delta 1$ and $\delta 2$. The difference of these two first difference spectra contains only the γ–δ correlations

$$F_{\gamma\delta}(Q) = \frac{\bar{b}^2 \Delta^2 F_{\gamma\delta}(Q)}{c_\gamma c_\delta (b_{\gamma 1} - b_{\gamma 2})\,(b_{\delta 1} - b_{\delta 2})}, \qquad (22)$$

where $\Delta^2 F_{\gamma\delta}(Q)$ represents the experimental double-difference spectrum.

3. Experiments

In section 2 the fundamentals of neutron diffraction have been presented. This section is devoted to showing what procedures are necessary to correct the experimental data. These corrections intend to take into account the approximations made to extract the data.

3.1. Corrections

There are two kind of corrections to be performed on the experimental data: one set coming from the experimental conditions and the other from the theoretical assumptions made to derive the structure factors. There are more or less standard programs to perform these corrections, for example the code CORRECT [10].

The main experimental correction is the background subtraction, for which it is necessary to measure the empty cell, the empty instrument and a sample-like absorbent. The knowledge of dimensions and materials of each component in the beam allows the calculation of the absorption coefficients and the extraction of the background-corrected spectrum for the sample. In the case of cylindrical geometry, these absorption coefficients can be calculated using the Paalman and Pings corrections [11]. Because of the finite size of the sample, there is always a probability that a neutron has more than a single interaction in the sample. This contribution, known as multiple scattering, must be evaluated and subtracted from the experimental data. This contribution can be evaluated using the Blech and Averbach correction [12]. For some kinds of molecular systems, for which a model of interaction between the neutrons and the scatterers can be used, it is better to use numerical simulations to evaluate the absorption/background and multiple scattering corrections [13].

The last experimental correction to perform is the correction for the instrumental resolution. Knowing the instrumental resolution, one can attempt to extract the structure factor by performing a deconvolution process, but this is a difficult task. Instead, one can measure a standard vanadium sample (an almost incoherent scatterer), which should give a flat diffractogram. In fact, this diffractogram is not flat because of the resolution of the instrument. Then the resolution-corrected data are obtained by taking the ratio between the sample diffractogram and that for vanadium. In doing this, and because the cross section of vanadium is well known, the data can be normalized to an absolute scale.

Finally, the last correction that must be performed concerns the inelasticity effects, originating from the fact that in a real experiment the scattering is not completely elastic, as assumed for the diffraction case. It is evident that this effect is more important for light atoms than for heavy ones and it is evidenced as a decrease in the intensity with Q. This can be described with a mass expansion of the cross section [14] or, in a more empirical way, by an even polynomial in Q.

Once the experimental double differential cross section has been converted into the total structure factor, the Fourier sine transform (equation (17)) must be done. In fact, due to the finite Q-range of any experimental diffractogram there will be always a high frequency noise in the pair distribution function (see the oscillations below 2 Å in figure 2). This effect can be reduced using window functions like that proposed by Lorch [15].

3.2. Instruments

When studying the structure of disordered materials there are basically two ways of determining the structure factor. The first one is using a two-axis diffractometer, which is usually installed in a steady state (reactor) neutron source. In this case, the Maxwellian distribution of neutron energies is monochromatized, focused on the sample and detected as a function of the scattering (2θ) angle (figure 4(a)). By means of the Bragg's law ($Q = 4\pi/\lambda \sin\theta$), valid in the static approximation, the angular scale can be changed into the modulus of the scattering vector scale.

The second way to determine the structure factor is by the time-of-flight technique, which is available in pulsed neutron sources. In this case, a pulsed white beam is sent from the source to the sample (figure 4(b)). The scattered beam is then counted by a detector placed at a constant scattering angle as a function of time of flight (t). If the total flight path is L, and using again the Bragg's law ($Q = 2mL/\hbar t \sin\theta$, where m is the neutron mass), it is possible to change from t- to Q-scale.

There are several instruments dedicated to the study of amorphous materials. For instance, at the Institut Laue

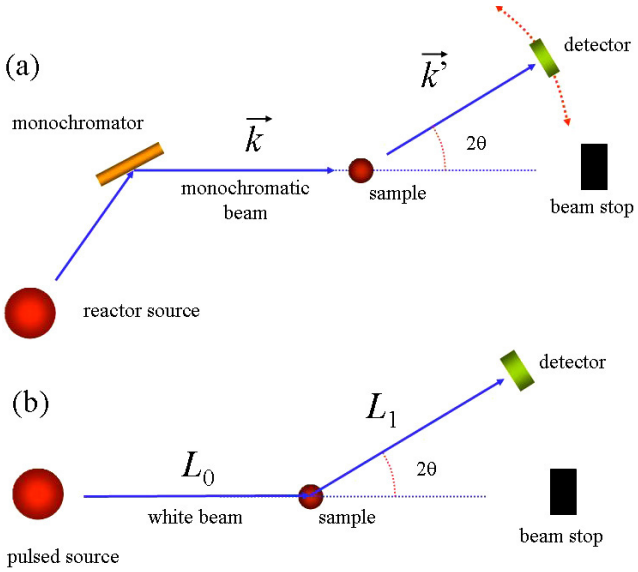

Figure 4. (a) Experimental layout of a two-axis diffractometer, where the beam is continuous and monochromatic and the diffractogram is collected as a function of the scattering angle. (b) Experimental layout of a time-of-flight diffractometer, where the beam is pulsed and white and the diffractogram is collected as a function of the time of flight.

Langevin (ILL) there is a large suite of instruments for structural and dynamical studies on non-crystalline solids [16]. In particular, for structural studies the available instruments in steady state sources are D4 [17] (ILL) and 7C2 [18] (LLB). The pulsed-source neutron diffractometers are SANDALS [19] (ISIS), GEM [20] (ISIS), HIT [21] (KENS) and GLAD [22] (IPNS).

4. Selected examples

These examples intend to illustrate some of the above discussed methods. First, a total structure factor determination is presented, where the combination of neutron diffraction and numerical simulation allows the obtention of structural information. Then an example of H/D substitution is given, where the intermolecular structure of glassy alcohols is derived. The structure of telluride glasses is derived combining neutron and x-ray diffraction and using the advantages of each technique for extracting information on the partial structure factors. Finally, we present an example where the isomorphic substitution technique allows us to study the short-range order of rare-earth ions in phosphate glasses.

4.1. Chalcogenide glasses

This is a case where a simple total structure factor determination has been performed without any isotopic substitution. The correlation distances in chalcogenide glasses were studied by means of a neutron diffraction experiment on the system $Ag_x(Ge_{0.25}Se_{0.75})_{100-x}$ with different silver contents ($x = 15$ and 25 at.%) [26]. This is a total structure factor determination, where the changes in the structure of the Ge–Se network upon doping with Ag were determined. The total structure factor $S(Q)$ for the two samples was measured at the two-axis diffractometer D4 (ILL) [17]. These two structure factors, where all the correlations are mixed in a single curve, were Fourier transformed to obtain the total correlation functions and their corresponding radial distribution functions. Because there is no isotopic substitution, the interpretation of the correlation functions must be done with the help of numerical simulations. In this way it was possible to identify the presence of both Se–Se and Ge–Se correlations in the first peak of the radial distribution functions. The results are consistent with a structure that contains both $GeSe_{4/2}$ tetrahedra and Se–Se bonds and Ag bonded to Se in a triangular coordination. The observed changes with temperature in the Ag–Ag correlation peak (at 3 Å) are in agreement with increased diffusion of silver throughout the glasses, even though they are much less drastic than those reported previously for a similar study on $Ag_{25}(Ge_{0.25}Se_{0.75})_{75}$ glass at higher temperatures.

4.2. Glassy alcohols

This is an example of a simple experiment where the total structure factors for both isomers of propanol were determined by neutron diffraction [23]. This example serves to illustrate how minor details of chemical structure may induce changes in ordering patterns at scales well beyond those where one would expect such changes to be strongest, that is at scales involving chemical and topological short-range order: in this case, the structures of the two isomers of propyl alcohol ($CD_3CD_2CD_2OD$ and $CD_3CDODCD_3$, 1-propanol and 2-propanol, respectively), which differ by the location of the hydroxyl group (figure 5). Such a minute difference in molecular structure results in large changes in basic thermal properties, such as the crystal melting points ($T_m = 148$ and 185 K, respectively), the glass-transition temperatures ($T_g =$ 98 and 115 K) and even the macroscopic liquid densities, that differ by some 2%.

The intermolecular structure of both glasses shows that the oscillations versus a rescaled variable (rescaled by a characteristic distance) are fully in phase. In other words, the intermediate range order is understandable in terms of packing of spherical entities defined by a characteristic radius r_m. Such positional correlations, which are fully identifiable with those of the molecular centers of mass, extend to a far larger extent than those of orientational origin, which tend to die out for distances just above r_m. Evidence of order even beyond the intermediate range has been observed in other glasses [24], simpler than these molecular glasses.

The total pair static correlation functions for 1-propanol show a very clear phase relationship between the oscillations of glass and crystal, indicating that the short-range structures of glass and crystal should show some resemblance. On the other hand, those for 2-propanol show rather disparate patterns. Such distinct behaviors were studied by means of high-resolution powder diffraction on the crystal structures of both isomers [25].

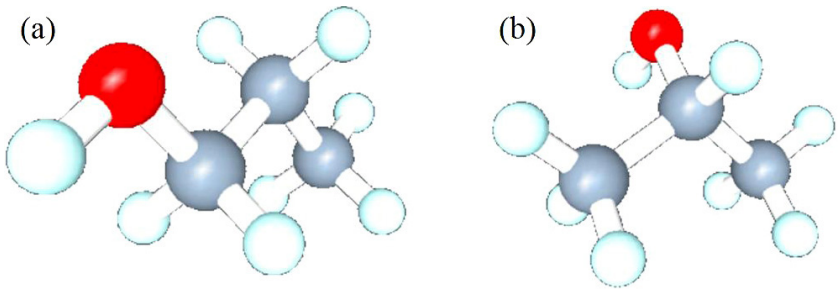

Figure 5. The two isomers of propanol: (a) 1-propanol and (b) 2-propanol.

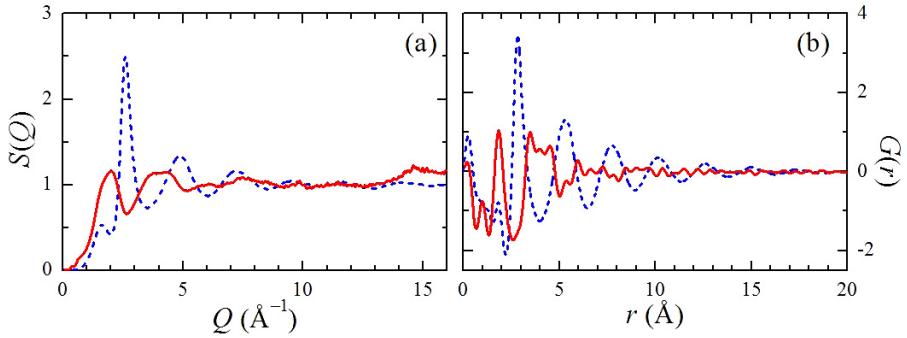

Figure 6. (a) The static structure factor of glassy $(Li_2O)_2$–$(TeO_2)_2$ − V_2O_5 as obtained from x-ray (solid line) and neutron (dashed line) diffraction experiments [28]. (b) The corresponding pair correlation functions (solid line, x-rays; dashed line, neutrons).

4.3. Tellurite glasses

Tellurium dioxide (TeO_2 or paratellurite) is a conditional glass former, which means it will form a glass with small molar% additions of a second compound such as an oxide or halide. This is the case of the binary TeO_2–V_2O_5 system, exhibiting a wide glass-forming region [27] and semiconducting properties with relatively high conductivity ($Te_2V_2O_9$ exhibits the highest conductivity). The ternary M_2O–$Te_2V_2O_9$ (M = Li, Na, Ag) system presents a continuous change from the pure electronic conductivity ($Te_2V_2O_9$) to a mainly ionic conductivity for high M_2O content. In the following example, neutron and x-ray diffraction techniques are combined to study the local structure of the ternary Li_2O–TeO_2–V_2O_5 system [28].

Three samples in the ternary $(Li_2O)_x$–$(TeO_2)_2$–V_2O_5 system with $x = 0$, 1 and 2 were measured. The neutron diffraction experiments were conducted on the D4 two-axis diffractometer at ILL [17] and the x-ray experiments were performed with a conventional laboratory diffractometer. Figure 6(a) shows the structure factors as obtained by neutron and x-ray diffraction for the glass with the highest Li content, i.e. $Li_4Te_2V_2O_{11}$, and figure 6(b) shows the corresponding pair coordination functions.

The joint neutron and x-ray scattering experiments allow us to obtain information about partial Te–O and V–O correlations for the $Te_2V_2O_9$ glass. Namely, the Te–O contribution can be estimated from the neutron data, for which the V–O component is very weak (the coherent scattering length is almost null). Then the V–O nearest-neighbor interatomic distances and the coordination numbers can be derived from the x-ray data, fixing the parameters for Te–O obtained from the neutron data in the fitting procedure. However, when the Li–O correlations are merged in the nearest-neighbor peak, a few additional assumptions about some of the parameters have to be made. The deconvolution of total correlation function in the case of Li-based glasses is more difficult. In the case of neutron scattering, even if the vanadium contribution can be negligible, the lithium one is important and negative. Thus it is difficult to refine Te–O and Li–O contributions together because they are correlated: an increase of one of them is compensated by the increase of the other one, and no change is observed in the experimental data. In this case the use of x-ray data is crucial, because the Li contribution to the correlation function is negligible, and V–O and Te–O are both positive. In this manner, the fitted results for V–O and Te–O correlations are kept fixed when Li correlations are refined in the neutron data. All the parameters are finally refined to obtain convergence and the result is checked with the x-ray data. Such a procedure is applied until a convergence is reached. More details of this method can be found in Rozier *et al* [28].

4.4. Anomalous scattering

Recently, the first successful complete neutron diffraction anomalous dispersion experiment was performed in order to investigate the role of the Sm^{3+} ions in the structure of vitreous $Sm_2O_3{\cdot}4P_2O_5$ [7, 8]. The ideal form of this technique, which employs the wavelength dependence of the real and imaginary parts of the neutron scattering length close to an absorption resonance, is used and involves measurements at two pairs of wavelengths: the real part of the scattering length is varied, keeping the imaginary part constant, and then the

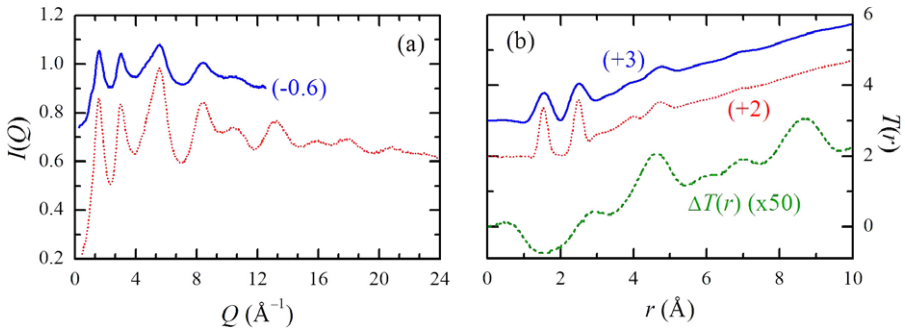

Figure 7. (a) The corrected diffraction patterns corresponding to $Sm_2O_3{\cdot}4P_2O_5$ at two wavelengths: 0.9 Å (top) and 0.45 Å (bottom). (b) The real-space correlation functions, $T(r)$, for the same two wavelengths and their corresponding difference correlation function, $\Delta T(r)$, as obtained by varying the imaginary part of the neutron scattering length.

imaginary part is varied, keeping the real part constant. If A denotes the element with the isotope (^{149}Sm) having the absorption resonance and X any other element present in the sample, the first measurement can be used to extract the A–A + A–X or A–A + X–X contribution to the real-space correlation function, $T(r)$, and the second yields the A–A component correlation function. Figure 7(a) shows the neutron diffraction pattern for two of the five wavelengths used in this experiment, i.e. 0.9 Å (upper curve) and 0.45 Å (bottom curve). The big difference in the measured intensity is caused by the energy dependence of the absorption cross section and the different Q-range is due to the fixed angular range of the diffractometer [17], i.e. 140°. Figure 7(b) shows the $T(r)$ function for these two wavelengths and their difference $\Delta T(r)$, from which the Sm–Sm + Sm–X contributions (X = P or O) are derived. For the present glass, these correlations reveal that the Sm^{3+} ions have an average coordination number, $n_{Sm(O)} = 7$, with a mean Sm–O bond length of 2.3757 ± 0.005 Å, while the anomalous difference correlation function indicates that the Sm^{3+} ions are ≈4.6 Å apart.

4.5. Rare-earth phosphate glasses

This is an example where the method of isomorphic substitution in neutron diffraction is applied to investigate the effect of rare-earth ion size on the structure of two (R_2O_3)–(Al_2O_3)–(P_2O_5) glasses prepared by using the same method. Specifically, neutron diffraction is used to study the structure of glassy $RAl_{0.30}P_{3.05}O_{9.62}$, which contains small R^{3+} ions (Dy^{3+} or Ho^{3+}) of radius 0.91–0.90 Å [29], and glassy $RAl_{0.34}P_{3.20}O_{10.04}$, which contains large R^{3+} ions (La^{3+} or Ce^{3+}) of radius 1.16–1.14 Å [30]. Isomorphic structures are assumed to result from the Dy/Ho or La/Ce substitution and difference function methods are then employed to separate, essentially, those correlations involving R^{3+} from the remainder [31]. Figure 8 shows the static structure factors for the six samples: that of $LaAl_{0.36}P_{3.32}O_{10.25}$ has been measured at GLAD [22] and the other at D4 [17]. The results show a rich structural complexity, which can be rationalized on the basis of the Hoppe *et al* model [32, 33] by treating both R^{3+} and Al^{3+} as network modifying cations.

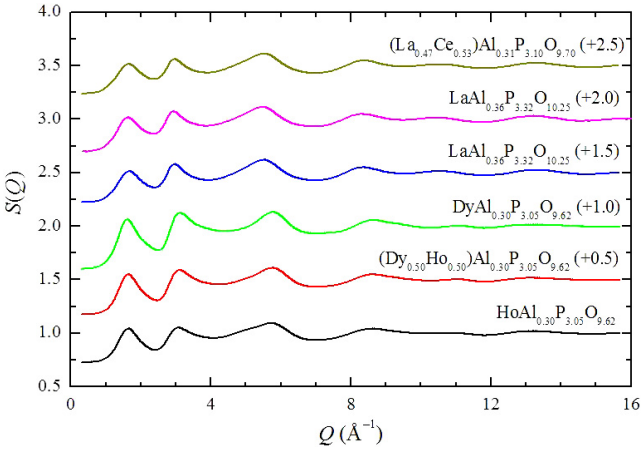

Figure 8. The static structure factors of glassy rare-earth phosphates. The three bottom curves correspond to the smaller rare earths (Dy and Ho), while the three top curves correspond to larger rare earths (La and Ce).

5. Conclusions

This article shows that, despite the complexity involved in the studies of short-range order in disorder materials, the use of special techniques allows us to extract the local structure around a given atom. The main difficulty in solving the structure of amorphous materials is that all the spatial correlations are collapsed in the same one-dimensional diffractogram. In general, neutron diffraction is the main tool to study the structure of glasses, thanks to the isotopic substitution method. Here it was shown that other less-conventional techniques can be very useful, such as isomorphic substitution, anomalous dispersion or combination of neutron and x-ray data. These same techniques can also be used to study liquids [3, 5, 6], solutions [34, 35] or even solid minerals [36, 37], where the order around a given atom is important.

This article was focused on the structural study of amorphous systems, but it is worth noticing that the main characteristic of thermal neutrons is that they allow us to study simultaneously the structure and dynamics of amorphous systems [16]. It is necessary to note that for dynamical studies

the techniques of isotopic or isomorphic substitution must be used carefully, due mainly to the difference in the mass of the substituted atoms.

Acknowledgments

I would like to thank P Palleau (ILL) for his technical support during the neutron diffraction experiments. I wish to thank P S Salmon, R A Martin, P Rozier, A Burian, A Piarristeguy, A Pradel, F J Bermejo, A C Wright and J M Cole for the use of their data collected at D4 (ILL).

References

[1] Squires G L 1978 *Introduction to the Theory of Thermal Neutron Scattering* (Cambridge: Cambridge University Press)
[2] Sears V F 1992 *Neutron News* **3** 26
[3] Dahlborg U, Besser M, Calvo-Dahlborg M, Cuello G J, Dewhurst C, Kramer M J and Sordelet D 2007 *J. Non-Cryst. Solids* **353** 3005
[4] Egelstaff P A 1967 *An Introduction to the Liquid State* (London: Academic) chapters 6 and 9
[5] Cuello G J, Fernández-Perea R, Cabrillo C, Bermejo F J and Román-Ross G 2004 *Phys. Rev.* B **69** 094201
[6] Cuello G J, Fernández-Perea R, Bermejo F J, Román-Ross G and Campo J 2007 *J. Non-Cryst. Solids* **353** 2987
[7] Wright A C, Cole J M, Newport R J, Fisher C E, Clarke S J, Sinclair R N, Fischer H E and Cuello G J 2007 *Nucl. Instrum. Methods Phys. Res.* A **571** 622
[8] Cole J M, Wright A C, Newport R J, Sinclair R N, Fischer H E and Cuello G J 2007 *J. Phys.: Condens. Matter* **19** 056002
[9] Fischer H E, Barnes A C and Salmon P S 2006 *Rep. Prog. Phys.* **69** 233
[10] Howe M A, McGreevy R L and Zetterström P 1996 *Computer Code CORRECT: Correction Program for Neutron Diffraction Data* NFL Studsvik
[11] Paalman H H and Pings C J 1962 *J. Appl. Phys.* **33** 2635
[12] Blech I A and Averbach B L 1965 *Phys. Rev.* **137** A1113
[13] Rodríguez Palomino L A, Dawidowski J, Blostein J J and Cuello G J 2007 *Nucl. Instrum. Methods Phys. Res.* B **258** 453
[14] Placzek G 1952 *Phys. Rev.* **86** 377
[15] Lorch E A 1969 *J. Phys. C: Solid State Phys.* **2** 229
[16] Cuello G J, Jiménez-Ruiz M and González M A 2007 *J. Non-Cryst. Solids* **353** 724
[17] Fischer H E, Cuello G J, Palleau P, Feltin D, Barnes A C, Badyal Y S and Simonson J M 2002 *Appl. Phys.* A **74** S160
[18] Ambroise J P, Bellissent-Funel M C and Bellissent R 1984 *Rev. Phys. Appl.* **19** 731
[19] Soper A K 1989 *Advanced Neutron Sources 1988* (*IOP Conference Series* vol 97) ed D K Hyer (Bristol: IOP Publishing)
[20] Hannon A C 2005 *Nucl. Instrum. Methods* A **551** 88
[21] Fukunaga T, Misawa M, Fujikawa T and Satoh S 1993 *KENS Report-IX* p 16
[22] Ellison A J G, Crawford R K, Montague D G, Volin K J and Price D L 1993 *J. Neutron Res.* **1** 61
[23] Cuello G J, Talón C, Bermejo F J and Cabrillo C 2002 *Appl. Phys.* A **74** S552
[24] Salmon P S, Martin R A, Mason P E and Cuello G J 2005 *Nature* **435** 75
[25] Talón C, Bermejo F J, Cabrillo C, Cuello G J, González M A, Richardson J W Jr, Criado A, Ramos M A, Vieira S, Cumbrera F L and González L M 2002 *Phys. Rev. Lett.* **88** 115506
[26] Cuello G J, Piarristeguy A A, Fernández-Martínez A, Fontana M and Pradel A 2007 *J. Non-Cryst. Solids* **353** 729
[27] Denton E P, Rowson H and Stanworth J E 1954 *Nature* **173** 1030
[28] Rozier P, Burian A and Cuello G J 2005 *J. Non-Cryst. Solids* **351** 632
[29] Martin R A, Salmon P S, Fischer H E and Cuello G J 2003 *J. Phys.: Condens. Matter* **15** 8235
[30] Martin R A, Salmon P S, Benmore C J, Fischer H E and Cuello G J 2003 *Phys. Rev.* B **68** 054203
[31] Martin R A, Salmon P S, Fischer H E and Cuello G J 2003 *J. Non-Cryst. Solids* **345/346** 208
[32] Hoppe U, Walter G, Kranold R and Stachel D 2000 *J. Non-Cryst. Solids* **263/264** 29
[33] Hoppe U, Ebendorff-Heidepriem H, Neuefeind J and Bowron D T 2001 *Z. Naturf.* A **56** 237
[34] Badyal Y S, Barnes A C, Cuello G J and Simonson J M 2004 *J. Phys. Chem.* A **108** 11819
[35] Sobolev O, Cuello G J, Román-Ross G, Skipper N T and Charlet L 2007 *J. Phys. Chem.* A **111** 5123
[36] Pitteloud C, Powell D H, González M A and Cuello G J 2003 *Colloids Surf.* A **217** 129
[37] Sobolev O, Charlet L, Cuello G J, Gehin A, Brendle J and Geoffroy N 2008 *J. Phys.: Condens. Matter* **20** 104207